ELectronics EXpress

LETTER

IEICE Electronics Express, Vol.14, No.17, 1–7

A snapback-free reverse conducting IGBT with recess and floating buffer at the backside

Jia Qiang Xie[1a)], Li Ma[2], Wei Li[2], Yong Gao[1], and Ning Mei Yu[1]

[1] *Xi'an University of Technology and Department of Electronic Engineering, Xi'an 710048, China*

[2] *Xi'an University of Technology and Department of Applied Physics, Xi'an 710048, China*

a) *xjq1007@126.com*

Abstract: We propose two novel ways to alleviate the reverse conducting insulated gate bipolar transistor (RC-IGBT) snapback phenomenon by introducing the floating field stop layer with a lightly doped p-floating layer and recess structure at the backside. The floating field stop layer is submerged in the N-drift region and located several micrometers above the P^+ anode region, which would not degrade the blocking capability but can suppress the snapback phenomenon effectively. When the collector length exceeds 100 µm, the snapback voltage ΔV_{SB} of the floating field stop RC-IGBT with the p-floating layer can be less than 0.5 V. Furthermore, the recess structure at the backside can separate the N^+ short and P^+ anode region, which will be beneficial to eliminate the snapback. Finally, an RC-IGBT with a floating buffer layer and recess at the backside is proposed. Compared to the RC-IGBT featuring an oxide trench between the N^+ short and P^+ anode, the proposed one has utilized the simple recess structure to replace the costly oxide trench and achieved the identical characteristics simultaneously.

Keywords: floating field stop, IGBT, reverse-conducting, recess

Classification: Power devices and circuits

References

[1] M. Antoniou, *et al.*: "The semi-superjunction IGBT," IEEE Electron Device Lett. **31** (2010) 591 (DOI: 10.1109/LED.2010.2046132).

[2] H. Feng, *et al.*: "A new fin p-body insulated gate bipolar transistor with low miller capacitance," IEEE Electron Device Lett. **36** (2015) 591 (DOI: 10.1109/LED.2015.2426197).

[3] M. Antoniou, *et al.*: "Novel approach toward plasma enhancement in trench-insulated gate bipolar transistors," IEEE Electron Device Lett. **36** (2015) 823 (DOI: 10.1109/LED.2015.2433894).

[4] H. Takahashi, *et al.*: "1200 V reverse conducting IGBT," Proc. ISPSD (2004) 133 (DOI: 10.1109/WCT.2004.239844).

[5] M. Rahimo, *et al.*: "The Bi-mode insulated gate transistor a potential technology for higher power applications," Proc. ISPSD (2009) 283 (DOI:

DOI: 10.1587/elex.14.20170677
Received June 29, 2017
Accepted July 24, 2017
Publicized August 17, 2017
Copyedited September 10, 2017

10.1109/ISPSD.2009.5158057).
[6] W. Zhang, *et al.*: "Increase of the reliability of the junction terminations of reverse-conducting insulated gate bipolar transistor by appropriate backside layout design," IEEE Electron Device Lett. **35** (2014) 1281 (DOI: 10.1109/LED.2014.2364301).
[7] M. Rahimo, *et al.*: "Thin-wafer silicon IGBT with advanced laser annealing and sintering process," IEEE Electron Device Lett. **33** (2012) 1601 (DOI: 10.1109/LED.2012.2215304).
[8] R. Kamibaba, *et al.*: "Next generation 650 V CSTBTTM with improved SOA fabricated by an advanced thin wafer technology," Proc. ISPSD (2015) 29 (DOI: 10.1109/ISPSD.2015.7123381).
[9] M. Antoniou, *et al.*: "A new way to alleviate the RC-IGBT snapback phenomenon: The superjunction solution," Proc. ISPSD (2010) 153.
[10] L. Storasta, *et al.*: "A comparison of charge dynamics in the reverse conducting RC-IGBT and Bi-mode insulated gate transistor BIGT," Proc. ISPSD (2010) 391.
[11] L. Storasta, *et al.*: "The radial layout design concept for the Bi-mode insulated gate transistor," Proc. ISPSD (2011) 56 (DOI: 10.1109/ISPSD.2011.5890789).
[12] L. Zhu and X. Chen: "An investigation of a novel snapback-free reverse-conducting IGBT and with dual gates," IEEE Trans. Electron Devices **59** (2012) 3048 (DOI: 10.1109/TED.2012.2215039).
[13] H. Jiang, *et al.*: "Band-to-band tunneling injection insulated-gate bipolar transistor with a soft reverse-recovery built-in diode," IEEE Electron Device Lett. **33** (2012) 1684 (DOI: 10.1109/LED.2012.2219612).
[14] H. Jiang, *et al.*: "A snapback suppressed reverse conducting IGBT with a floating p-region in trench collector," IEEE Electron Device Lett. **33** (2012) 417 (DOI: 10.1109/LED.2011.2180357).
[15] U. Vemulapati, *et al.*: "Reverse conducting IGBTs initial snapback phenomenon and its analytical modelling," IET Circuits Dev. Syst. **8** (2014) 168 (DOI: 10.1049/iet-cds.2013.0222).
[16] W. Hsu, *et al.*: "Reverse-conducting insulated gate bipolar transistor with an anti-parallel thyristor," Proc. ISPSD (2010) 149.

1 Introduction

The insulated gate bipolar transistor (IGBT) is now one of the most attractive power devices due to the continuous innovations and comprehensive enhancements of performance. The IGBT is indispensable for many power electronic equipment, for example, traction, motor control, and induction heating [1, 2, 3]. In most cases, the IGBT needs to connect with an anti-parallel free-wheeling diode (FWD) for reverse conduction. In order to improve the power handling capability of the IGBT modules, an attractive approach is to incorporate the FWD and IGBT into a monolithic silicon chip [4]. Such solution has been implemented and then the RC-IGBT appears in the market partly due to the thin-wafer processing technology in recent years [5, 6, 7, 8]. Compared to the conventional IGBT configuration, the RC-IGBT features periodic and alternating N^+ short region and P^+ anode region at the backside. The N^+ short regions in RC-IGBTs act as the cathode of the internal integrated FWD during the reverse conduction state. However, in the forward state the current would initially flow through the N^+ short region rather than the P^+

DOI: 10.1587/elex.14.20170677
Received June 29, 2017
Accepted July 24, 2017
Publicized August 17, 2017
Copyedited September 10, 2017

anode. That is to say, there were no hole injections from the P^+ anode, and the conductivity modulation of the drift region cannot take place until the anode p-n junction at the backside is forward biased. Only when the anode voltage exceeds some critical value could the operation of the IGBT mode occur. Such a problem is called snapback phenomenon.

Recently, several structure have been proposed such as the SJ-RC-IGBT, the AG-RC-IGBT, the band to band tunneling injection IGBT and so on. The SJ-RC-IGBT eliminated the snapback by decrease the resistance of the drift. The AG-RC-IGBT can work at different modes by the control of the backside gate. The band to band tunneling injection IGBT realizes the reverse conduction capability by the band to band tunneling mechanism [9, 10, 11, 12, 13]. The RC-IGBT with a floating p-region and an oxide trench between the N^+ short and P^+ anode [14], which would be referred to as OT-RC-IGBT in this paper. By utilizing the numerical simulation, this paper proposes a simple way to suppress the snapback by introducing the floating field stop layer with a lightly doped p-floating layer. The new technology is referred to as the floating field stop reverse-conducting IGBT (FFS-RC-IGBT) and implying that the device features a gap layer between the field stop layer and the P^+ anode. Thus, a higher resistivity layer above the P^+ anode is achieved to initiate the hole injection from the P^+ anode at low currents. The gap layer above the P^+ anode, which has the same light doping concentration with the N-drift region, could help to suppress the snapback voltage of the RC-IGBT. Additionally, if a lightly doped p-floating layer is formed below the floating field stop, the new one would contribute more significant effect in the suppression of the snapback phenomenon.

This paper also proposes a novel structure, which is named recess and floating buffer RC-IGBT (RF-RC-IGBT). Compared to the OT-RC-IGBT structure described in [14], a simple recess configuration is used to replace the oxide trench, and the floating buffer structure is also utilized to suppress the snapback phenomenon and achieve sufficient blocking capability.

2 FFS-RC-IGBT structure

Fig. 1(a) and (b) show the schematic cross-section of the conventional RC-IGBT and the proposed FFS-RC-IGBT, respectively. As can been seen from Fig. 1(b) that the introduced N-drift-gap layer raise the N-buff layer to form the floating field stop layer structure. In order to further eliminate the snapback phenomenon, a low doped thin p-floating layer is added between the N-drift gap layer and floating

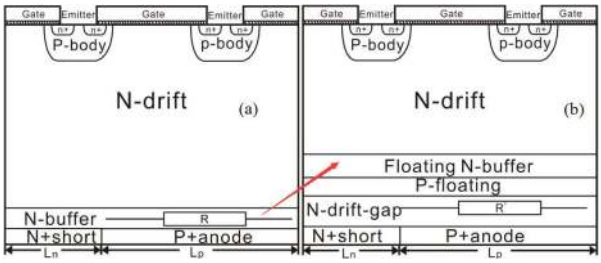

Fig. 1. (a) The conventional RC-IGBT and (b) the FFS-RC-IGBT.

DOI: 10.1587/elex.14.20170677
Received June 29, 2017
Accepted July 24, 2017
Publicized August 17, 2017
Copyedited September 10, 2017

N-buffer layer. The thickness of N-drift-gap layer is 1 μm. It is located above the P^+ anode. In a word, the floating field stop layer consist of the p-floating layer and the N-buff layer. By introducing the p-floating layer and N-drift-gap layers, the RC-IGBT snapback phenomenon is effectively suppressed.

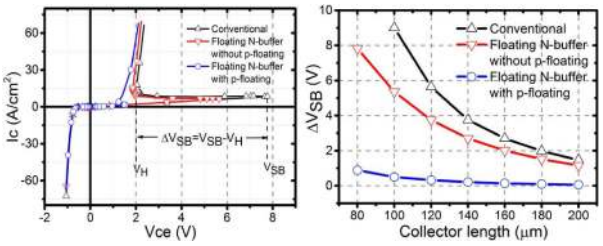

Fig. 2. (a) The comparison of on-state characteristics (b) Influence of collector length on snapback voltage.

These RC-IGBTs, whose collector lengths are all equal to 120 μm. Fig. 2(a) illustrates the on-state characteristics of the three RC-IGBTs when the doping concentration of the p-floating layer in FFS-RC-IGBT is 7×10^{14} cm^{-3}. The snapback voltage ΔV_{SB} ($= V_{SB} - V_H$) of the FFS-RC-IGBT with p-floating layer is 0.32 V, whereas the conventional one is 5.64 V which indicating that snapback can be eliminated when the floating field stop with p-floating layer structure is used. As Fig. 2(b) shows, the ΔV_{SB} will be reduced when the collector length (Lp + Ln) is increased. This phenomenon indicates that large device sizes can effectively reduce ΔV_{SB}. It should be noted that the ratio of the width Ln and Lp is 1:4 for all collector sizes. However, the snapback voltage ΔV_{SB} of the proposed RC-IGBT has been always smaller than that of the conventional one. As expected, the snapback phenomenon is mainly determined by the width of the P^+ anode Lp and is not dependent on the width or the proportion of N^+ short Ln [15]. It means that when Ln/Lp tends to zero, RC-IGBT will become the traditional IGBT, which completely eliminates the snapback phenomenon. The structure parameters are listed in Table I.

Table I. The device parameters

Variable	Conventional	FFS-IGBT (without P-floating)	FFS-IGBT (with P-floating)
N-buffer thickness (m)	2	2	2
N-buffer doping cm^{-3}	2e16	2e16	2e16
P-floating thickness (μm)	/	/	1
P-floating doping cm^{-3}	/	/	7e14
N-buffer-gap thickness (μm)	/	2	1
N-buffer-gap doping cm^{-3}	/	7e13	7e13

The collector lengths of the p-floating layer are all equal to 180 μm. It can be seen from Fig. 3 that snapback voltage depends on the doping concentration of the p-floating layer and the reverse conduction does not depend on that doping. However, it should be noted that when the doping concentration of the p-floating layer exceeds 9×10^{14} cm^{-3}, the device occurs punch-through effect between the

DOI: 10.1587/elex.14.20170677
Received June 29, 2017
Accepted July 24, 2017
Publicized August 17, 2017
Copyedited September 10, 2017

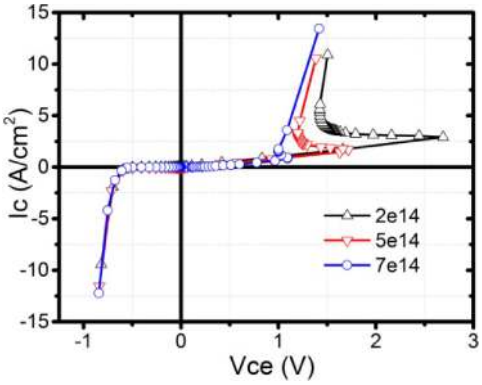

Fig. 3. On-state characteristics of the FFS-RC-IGBT with different doping concentrations of the p-floating layer.

p-floating and P^+ anode. Therefore, the N^+ short layer is isolated. At that case, the FFS-RC-IGBT acts as conventional IGBT. Then, reverse voltage induced avalanche breakdown between the p-float and the floating n-buffer. Moreover, the floating field stop structure does not compromise the blocking voltage capability at all. The blocking characteristic will be discussed in the next section.

3 RF-RC-IGBT structure

The schematic cross-section of OT-RC-IGBT and RF-RC-IGBT is illustrated in Fig. 4(a) and (b), respectively. The emitter sides of both structures are identical to the conventional IGBT. The backside of the RF-RC-IGBT, however, uses a recess structure to separate the N^+ short and P^+ anode rather than the oxide trench in OT-RC-IGBT. The lifetimes of electron and hole are set to 10 µs and 3 µs, respectively. The structure parameters are listed in Table II.

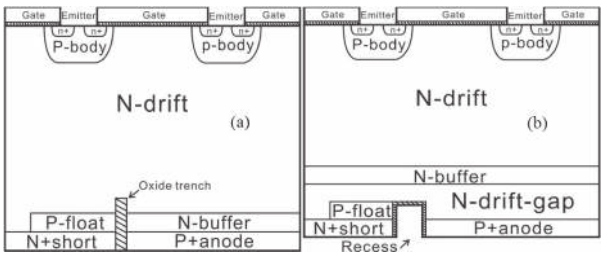

Fig. 4. The cross section of ((a) OT-RC-IGBT) and ((b) RF-RC-IGBT).

As it can be seen from Fig. 4(a) that a floating p-region and an oxide trench between the N^+ short and P^+ anode and (b) the proposed RF-RC-IGBT with floating buffer and the recess structure, which is utilized to isolate the N^+ short and P^+ anode. The thickness of the thin oxide layer on the inner surface of the recess is 100 nm. Moreover, the floating N-buffer is embedded in the N-drift region and located 4 µm above the P^+ anode. In Fig. 4(b), the P-float sandwiched between the N^+ short and N-drift-gap layer functions as a potential barrier for electrons during the initial forward conduction, just like the narrow P^- layer in RC-IGBT described in [16] or the P-float in OT-RC-IGBT. The effect of varying the P-float doping on the snapback voltage is investigated. The structure parameters are listed in Table II.

DOI: 10.1587/elex.14.20170677
Received June 29, 2017
Accepted July 24, 2017
Publicized August 17, 2017
Copyedited September 10, 2017

Table II. The device parameters

Variable	OT-RC-IGBT	RF-RC-IGBT
Half cell width (μm)	40	40
N-drift thickness (μm)	120	120
N-drift doping cm^{-3}	7e13	7e13
N-buffer thickness (μm)	2	2
N-buffer doping cm^{-3}	2e16	2e16
Oxide trench depth (μm)	5	/
Oxide trench width (μm)	1	/
Recess depth (μm)	/	4
Recess width (μm)	/	3
N-drift-gap thickness (μm)	/	4
N-drift-gap doping cm^{-3}	/	7e13
N^+ short length Ln (μm)	10	8
N^+ short thickness (μm)	2	2
N^+ short doping cm^{-3}	1e19	1e19
P^+ anode length Lp (μm)	29	29
P^+ anode doping cm^{-3}	4e17	4e17
P-float length (μm)	9	7
P-float thickness (μm)	2	2
P-float doping cm^{-3}	1e16	1e16

4 RF-RC-IGBT characteristics and discussion

Fig. 5(a) shows the influence of P-float doping concentration on forward conduction characteristics in RF-RC-IGBTs. The higher the P-float doping, the smaller the snapback voltage, as the electric potential barrier between N^+ short and P-float will be increased accordingly.

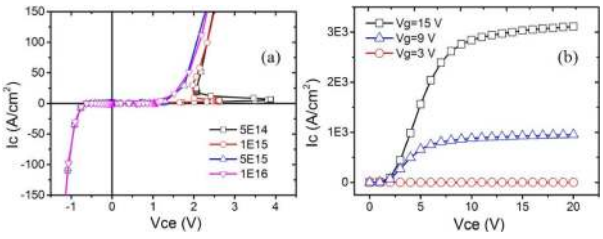

Fig. 5. (a) Snapback voltage with different P-float layer doping concentration of RF-RC-IGBT; (b) the on-state characteristics of the RF-RC-IGBT with the varying gate voltage.

When the P-float doping concentration exceeds 5×10^{15} cm^{-3}, the snapback effect can completely vanish. Without the use of the P-float layer and the recess structure, the snapback voltage ΔV_{SB} would be very large, and even the IGBT mode would never occur, which can be inferred from Fig. 2(b). Fig. 5(b) illustrates the output I-V characteristics of the proposed RF-RC-IGBT when the P-float doping is 1×10^{16} cm^{-3}. It should be noted that the doping of the P-float layer does not affect reverse conduction.

The blocking characteristics of these two RC-IGBTs are shown in Fig. 6. It can be seen that both of the breakdown voltage reached more than 1500 V, and the trend of breakdown characteristics curve is consistent. In contrast, there is no difference

DOI: 10.1587/elex.14.20170677
Received June 29, 2017
Accepted July 24, 2017
Publicized August 17, 2017
Copyedited September 10, 2017

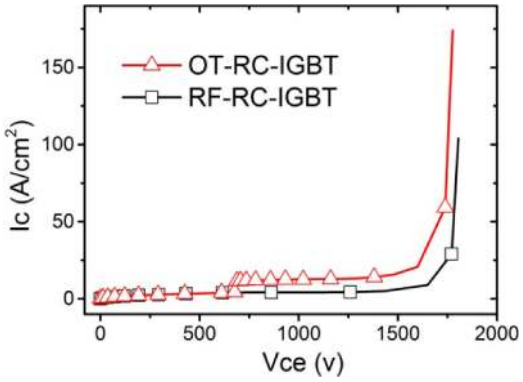

Fig. 6. Comparison of the blocking performance of the two RC-IGBTs.

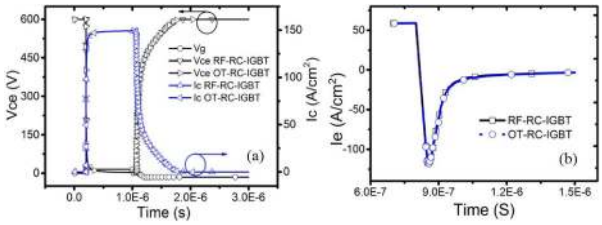

Fig. 7. (a) The switching characteristics. (b) The reverse recovery characteristic of the embedded diode for both RC-IGBTs.

in blocking capacity between the floating field stop structure and oxide trench structure. Fig. 7(a) and (b) depict the switching characteristics in IGBT mode and the reverse recovery in FWD mode, respectively. The value of resistance in the circuit is 100 Ω. The gate voltage is 15 V during the on state. The bus voltage is 600 V. As the Fig. 7(a) shows, the gate voltage start at the time = 0.2 μs. Then, the current I_c rises sharply until a steady value of 150 A/cm^2. At this stage, the forward voltage drop V_{ce} is almost zero. At the time = 1 μs, the gate voltage is turned off and the current I_c drops sharply. At this time, both the RC-IGBT turned off. The behavior of RF-RC-IGBT is similar to OT-RC-IGBT. Therefore, the dynamic characteristics have not been compromised by introducing the recess and floating buffer structure.

5 Conclusions

We have demonstrated that the floating field stop with a lightly doped p-floating layer and recess structure at the backside of the RC-IGBT can effectively suppress the snapback phenomenon when compared to a conventional RC-IGBT. Hence, there will be two additional design degrees of freedom by using recess structure and floating buffer in RC-IGBTs. More importantly, the recess structure can be fabricated to be more convenient than the oxide trench in the OT-RC-IGBT. It should be noted that the cell width of the proposed RF-RC-IGBT is just tens of micrometers and nearly one-tenth of the conventional one, thus, it will not produce the clutter current on the backside. In other words, the two proposed structures could overcome the trade-off between P^+ anode width Lp and N^+ short width Ln, which determine the initial snapback in forward conduction and current uniformity during reverse conduction, respectively.

DOI: 10.1587/elex.14.20170677
Received June 29, 2017
Accepted July 24, 2017
Publicized August 17, 2017
Copyedited September 10, 2017